Applicable Analysis
2011, 1–11, iFirst

Taylor & Francis
Taylor & Francis Group

Pattern quarks and leptons†

Alan C. Newell*

Department of Mathematics, University of Arizona, Tucson, AZ 85721, USA

Communicated by R.P. Gilbert

(*Received 25 August 2011; final version received 25 August 2011*)

Disclinations, concave and convex, are the canonical point defects of two-dimensional planar patterns in systems with translational and rotational symmetries. From these, all other point defects (vortices, dislocations, targets, saddles and handles) can be built. Moreover, handles, coupled concave–convex disclination pairs arise as instabilities, symmetry breaking events. The purpose of this article is to show that embedded in three or more dimensions, concave and convex disclination strings, two-dimensional disclinations with loop backbones, have interesting and suggestive invariant indices which are integer multiples of $\pm\frac{1}{2}$ and $\pm\frac{1}{3}$.

Keywords: disclinations; quarks; leptons

AMS Subject Classifications: 35B36

1. Introduction

One of the outstanding successes of modern physics has been the Standard Model [1]. It has provided a theoretical framework for combining the electromagnetic, weak and strong forces and for describing all currently known particles (the Higgs boson has yet to be observed) based on the building blocks of quarks and leptons. It does, however, suffer from a deficiency in that the symmetries SU(2) and SU(3), required for the notions of fractional spin and charge, are inserted by hand into the governing Lagrangian. Although I have no illusions that the story I shall tell in this brief article has much to add to our understanding of the behaviours of fundamental particles, it nevertheless should be of interest that there are systems, which begin with the simplest of symmetries, namely translation and rotation that give rise to fields containing objects with fractional invariants of 'spin' $\pm\frac{1}{2}$ and 'charge' $(\pm\frac{1}{3}, \pm\frac{2}{3})$ as a result of a spontaneous symmetry breaking of the original symmetries induced by an applied stress. None of these emerging structures are put into the theory, *a priori*, by hand.

The objects we discuss arise naturally in pattern forming systems and are three-dimensional structures closely related to the two-dimensional disclinations seen in

*Email: anewell@math.arizona.edu
†This article is dedicated to the memory of Alan Jeffrey, a pioneer in the asymptotic treatment of nonlinear waves.

ISSN 0003–6811 print/ISSN 1563–504X online

http://dx.doi.org/10.1080/00036811.2011.619983
http://www.tandfonline.com

Rayleigh–Benard convection at high Prandtl numbers [2], in ferrofluids [3] and in liquid crystals [4]. Indeed, after a recent lecture I gave in Goettingen about these ideas, I learned of a wonderful experiment which has just been reported in a recent issue of *Science* [5] (see also [6]) in which the authors demonstrate the knotting of topological defect lines in chiral nematic liquid crystal colloids which clearly have fractional invariants. They are also first cousins of the three-dimensional spiral or scroll waves observed in excitable chemical media [7] although the latter do have integer rather than fractional invariants connected with their well-defined circulations $\int_C \vec{k} \cdot \mathrm{d}\vec{x}$. To my knowledge, the only other example of fractionally charged quasiparticles is in the fractional quantum Hall effect [8,9].

In this article, we begin with stressed pattern forming systems which have stripes as their preferred planform and which have no soft or zero (Goldstone or 'mean drift') modes. We will show, first in two dimensions, how concave (V) and convex (X) disclinations spontaneously arise as instabilities and how they are solutions of the field equation which describes the macroscopic behaviour of the striped pattern. Their three-dimensional extensions, which we call V and X strings, are constructed by adding loop backbones to these structures in exactly the same manner that the twisted vortices are constructed in excitable media. We begin the story using a toy model for pattern forming systems, the Swift–Hohenberg (SH) equation [10] for the real field $\omega(\vec{x}, t)$,

$$\frac{\partial \omega}{\partial t} + (\nabla^2 + 1)^2 \omega - R\omega + \omega^3 = 0. \tag{1}$$

We start by summarizing briefly the Cross–Newell (CN) phase diffusion equation [10–13] which captures the slow and macroscopic dynamics of patterns far from equilibrium. The SH equation mimics qualitatively the patterns seen, for example, in Rayleigh–Benard convection at high Prandtl numbers in a horizontal layer of fluid heated from below. In (1), R is analogous to the difference between the Rayleigh number R_a and the onset value $(R_a)_c$ at which value the spatially uniform conduction state becomes unstable to striped convective patterns (rolls) which break the translational symmetry of the original system. R_a is a nondimensional measure of the temperature difference across the layer. We can think of the field $\omega(\vec{x}, t)$ in (1) as being the temperature or vertical velocity field at the middle of the layer. Roll solutions, the stable planform for $R > 0$, can be easily calculated as a 2π periodic Fourier cosine series

$$\omega(\vec{x}, t) = F(\theta; A_n(k, R), k, R) = \sum_{n=1}^{\infty} A_n(k, R) \cos n\theta, \tag{2}$$

where the phase $\theta(\vec{x}, t) = \vec{k} \cdot \vec{x} + \theta_0$ and $k = |\vec{k}| = 1$ is the preferred wavenumber (the 'one' with the Laplacian in (1)). The preferred wavelength is 2π. The direction of $\vec{k}$ is the direction normal to the roll axes. Because it does not matter whether we label the neighbouring constant phase contours corresponding to field maxima (minima) as 0, 2π, 4π or 0, -2π, -4π, the field must be even in θ. This fact also leads to some crucial topological features of pattern defects. The amplitudes $A_n(k, R)$ are slaved to the wavenumber k by algebraic relations.

Why do natural patterns have defects and why does one need to introduce the notion of phase variation and diffusion? The key realization is that whereas the

pattern planform (rolls) and pattern wavelength (2π) are chosen for energetic reasons, the rotational symmetry leaves open the choice of the roll direction $\vec{k}$. Indeed, in large boxes, (the inverse aspect ratio ε of the system is defined to be the ratio of the wavelength to the box size) where $0 < \varepsilon \ll 1$, local biases due to boundary conditions or variations in the bulk will determine the local orientations of the roll patches. These patches spread and, in two dimensions, they meet, merge and meld along line and at point defects. The line defects are called phase grain boundaries (PGBs) across which the phase is continuous but its gradient, the local wavevector changes direction. If the change in direction is too much, we show that a nipple instability occurs and leads to the creation of concave–convex point disclination pairs. An example of such a natural pattern in a ferrofluid is shown at the top right corner of Figure 1. The other parts of the figure show concave and convex disclinations in convection patterns and on counterpropagating light beams. The concave disclination on the lower right corner results from a simulation of the SH equation with carefully chosen boundary conditions. The coarsening of such patterns takes a very long time so for all intents and purposes they are stationary.

To describe such patterns analytically, we have to allow for the local wavevector $\vec{k}$ to change slowly almost everywhere in the bulk and also to allow for more sudden changes (shock like solutions) near point and line defects. CN theory [10–15], a derivative of Whitham [16] theory for waves, allows us to do this. We seek solutions $\omega(\vec{x}, t)$ which are modulations of (2),

$$\omega_0(\vec{x}, t) = F\left(\theta = \frac{\Theta(\vec{X}, T)}{\varepsilon}\right) = \sum_{1}^{\infty} A_n(k, R)\cos n\theta, \tag{3}$$

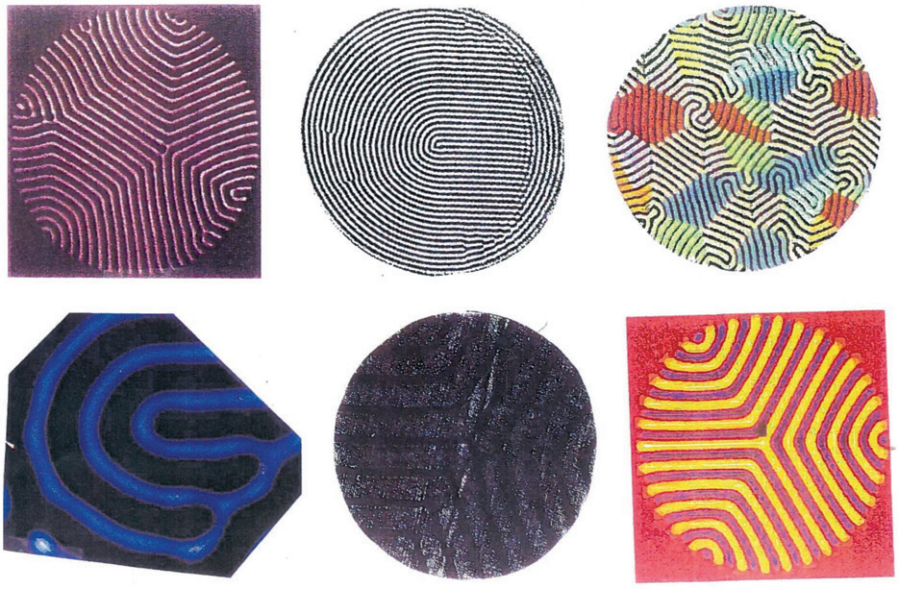

Figure 1. Concave–convex point disclinations in experiments.

where $\vec{X} = \varepsilon\vec{x}$, $T = \varepsilon^2 t$, $\vec{k} = \nabla_{\vec{x}}\theta = \nabla_{\vec{X}}\Theta$, and ε, $0 < \varepsilon \ll 1$ is the inverse aspect ratio and the small parameter in far from equilibrium situations. Because $\vec{k}(\vec{X}, T)$ changes, (3) is no longer an exact solution of (1) and corrections

$$\omega(\vec{x}, t) = \omega_0(\vec{x}, t) + \varepsilon\omega_1(\vec{x}, t) + \cdots \tag{4}$$

must be sought. Because of translational invariance, both $F(\theta)$ and $F(\theta + \delta\theta)$ are exact solutions of (1) to leading order. Therefore $\frac{\partial F}{\partial \theta}$ is a symmetry, meaning that it satisfies (1) linearized about $\omega = \omega_0$. This means that the equations for the iterates $\omega_1, \omega_2, \ldots,$ whose right-hand sides contain terms involving the variations of $\Theta(\vec{X}, T)$ and $\vec{k}(\vec{X}, T)$ with respect to the slow spatial variable and time, must satisfy certain solvability conditions which express constraints on the manner in which the order parameter $\vec{k} = \nabla\Theta$ of the macroscopic system can vary. These solvability conditions can be written as two asymptotic expansions. The first is the amplitude component which, at leading order, gives a system of nonlinear algebraic equations for $A_n(k, R)$ in terms of $A_1(k, R)$ and an algebraic equation for $A_1(k, R)$ in terms of k and R (roughly $(R - (k^2 - 1)^2)A_1 - \frac{3}{4}A_1^3 = 0$). Its corrections at ε^2, ε^4 involve time and space partial derivatives of A_1 and $\vec{k}$. They are only important when A_1 is small, that is, near onset when R is small. Near $R = 0$, they combine with the solvability conditions arising at odd powers of ε, the CN phase diffusion equation, to give the familiar Gingburg–Landau type Newell–Whitehead–Segel equation [17,18] for a complex order parameter $A = A_1 \exp i\theta$. Far from onset, however, there is only one-order parameter, the phase or phase gradient, and it satisfies

$$\tau(k)\frac{\partial\Theta}{\partial T} + \nabla \cdot \vec{k}B(k) + \varepsilon^2\eta\nabla^4\Theta = 0\,, \tag{5}$$

the regularized CN (RCN) equation. In (5), $\tau(k)$ is positive and η is calculable. The interesting structure is contained in the function $B(k)$ which, because of rotational invariance, only depends on k. It is defined for $k_L < k < k_R$, where $k_L(R)$ and $k_R(R)$ are the left- and right-hand boundaries of the neutral stability curve for the instability in (1) of the 'conduction' solution $\omega = 0$. The graph of $kB(k)$ is cubic in shape, zero at k_L, positive between k_L and k_0 and negative between k_0 and k_R. k_0 is the single internal zero of $kB(k)$ in (k_L, k_R) and here is equal to one, the preferred wavenumber. The graph has a maximum at $k = k_{EL}$ and a minimum at k_{ER}, called the Eckhaus stability boundaries. A little analysis shows that the second-order quasilinear partial differential expression $\nabla \cdot \vec{k}B$ in $\Theta(\vec{X}, T)$ is elliptic positive in (k_L, k_{EL}), hyperbolic in (k_{EL}, k_0), elliptic negative in (k_0, k_{ER}), a region called the Busse balloon and again hyperbolic in (k_{EL}, k_R). Since natural patterns have a wavenumber $k = k_0 = 1$ almost everywhere except at line and point defects, at the line and point defects the deviation from 1 is negative (see Figure 1). Therefore if one plots a histogram of wavenumbers in that class of natural patterns for which the SH equation is a useful model, one sees that it has its maximum at a wavenumber slightly below $k = k_0 = 1$. As a consequence, without the correction, Equation (5) is the reverse heat equation along the direction parallel to the local axis of the rolls. Therefore the correction biLaplacian is required in the vicinity of those regions where $k < k_0 = 1$ and plays a role entirely analogous to dissipation and diffusion in shock formation situations. It stops the unbounded amplification of small scales and leads to smooth transitions in the wavevector direction along PGBs.

2. Properties of (5) in two space dimensions

We now state several properties of Equation (5) in two spatial dimensions. The interested reader can consult the cited references [10–15] for more discussion.

(1) It is universal for all pattern forming systems assuming no soft modes, such as the mean drift we would find in moderate to low Prandtl number situations, are present. The graph of $kB(k)$ always has the cubic shape, positive between k_{EL} and k_0 and negative from k_0 to k_{ER}.

(2) It inherits the fact that (1) is gradient,

$$\tau(k)\frac{\partial\Theta}{\partial T} = -\frac{\delta E}{\delta\Theta}, \tag{6}$$

where

$$E = \int \left(G^2 + \varepsilon^2\eta(\nabla^2\Theta)^2\right)\mathrm{d}\vec{X} \tag{7}$$

and

$$G^2 = -2\int_{k_0=1}^{k} kB(k)\mathrm{d}k.$$

For (1),

$$4kB(k) = \frac{\mathrm{d}}{\mathrm{d}k}\int_0^{2\pi} F^4\mathrm{d}\theta.$$

Indeed $\frac{1}{\varepsilon}E$ is simply the free energy for (1) averaged over many wavelengths. It turns out that even though the Oberbeck-Boussinesq equations for high Prandtl number convection are not exactly gradient, the 'averaged' pattern behaves as if they were.

(3) Because in many circumstances the wavenumbers k throughout the region are close to the preferred wavenumber, one can often approximate G^2 by $(k^2-1)^2$. By rescaling, we can take $\eta = 1$. Then the free energy (7) divided by ε is

$$\frac{1}{\varepsilon}E = \int\left(\frac{1}{\varepsilon}(1-(\nabla\Theta)^2)^2 + \varepsilon(\nabla^2\Theta)^2\right)\mathrm{d}\vec{X} \tag{8}$$

which, after writing $\vec{X} = \varepsilon\vec{x}$, is exactly analogous to the sum of the strain and bending energies for thin elastic sheets with thickness proportional to ε and vertical deformation $\Theta(\vec{X}, T)$ [19].

(4) The connection between (8) and the family of Gingburg–Landau minimization problems is given in [15,20]. The challenges in dealing with nonconvex energies and the associated lack of uniqueness are discussed there.

(5) We will be searching for minimizers of (8) over fields $\Theta(\vec{X}, T)$ and gradients $\nabla\Theta$ which are double valued, namely director fields (vector fields without the arrow!) or vector fields over a double cover of the plane (in two dimensions). The reason for this is the property, mentioned earlier, that we can label neighbouring contours of constant phase as either increasing or decreasing by 2π. Mathematically, one can see that given a real field $\omega(\vec{x}, t) = A\cos\theta$

Figure 2. Concave disclination.

Figure 3. Convex disclination.

one can determine θ and $\nabla\theta$ from $\omega(\vec{x}, t)$ only up to sign. As a consequence, the point defects V, a concave disclination, and X, a convex disclination, shown in Figures 2 and 3, have the property that if one follows the 'wavevector' on any contour surrounding the point singularity, it twists by $-\pi$ or π. When divided by 2π, these invariant indices are analogous to spins of $\mp\frac{1}{2}$. The minimum energy configuration for a concave disclination will have angles of 120° between the angles of PGBs.

(6) The minimization of (7) has a wonderful self-dual property. Solutions of the self-dual equations

$$\varepsilon\nabla^2\Theta = \pm\sqrt{G^2} \simeq \pm\big(1 - (\nabla\Theta)^2\big) \tag{9}$$

are solutions of the full fourth-order Euler–Lagrange equation for (7) and (8), if the solution (level surface) $\Theta(\vec{X}, T)$ has zero Gaussian curvature. The Gaussian curvature for the PGBs and is always zero. For disclinations (Figures 2 and 3), it resides at the point singularity in each of their centres and is zero elsewhere.

(7) This property allows us to linearize the Euler–Lagrange equation via the transformation $\Theta = \varepsilon \ln\psi$ whence

$$\varepsilon^2\nabla^2\psi - \psi = 0. \tag{10}$$

Solutions such as $e^{\vec{k}_1\cdot\vec{X}/\varepsilon} + e^{\vec{k}_2\cdot\vec{X}/\varepsilon}$, $|\vec{k}_1| = |\vec{k}_2| = 1$ describe a PGB whose direction is $\frac{\vec{k}_1+\vec{k}_2}{2}$. If the PGB is $Y = 0$, then the exact minimizer for (8) is

$$\nabla\Theta = \cos\varphi, \quad \sin\varphi\tanh\left(\frac{Y}{\varepsilon}\sin\varphi\right), \tag{11}$$

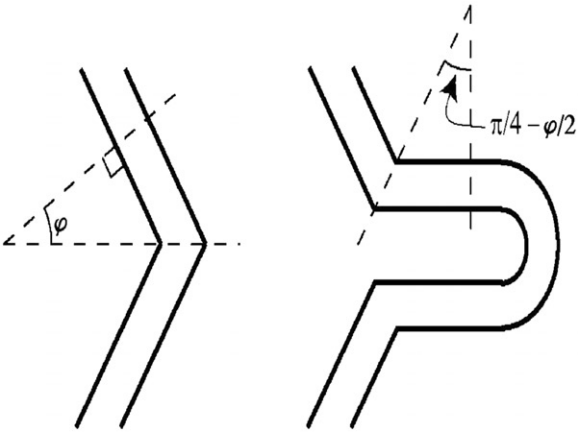

Figure 4. V and X disclination pair creation.

which is a vector field. In (11), φ is the angle between the wavevector ($\cos\varphi$, $\sin\varphi$) and the PGB (Figure 4). The energy of the PGB is proportional to $\sin^3\varphi$ per unit length of PGB. It is clear that this solution cannot continue to $\varphi = \frac{\pi}{2}$ because simply relabelling maximum θ contours as 4π, 2π, 0, 2π, 4π should not cost anything.

(8) Indeed, for large angles φ, (11) is unstable because a lower energy minimum can be found by introducing a director field perturbation which creates two disclinations, a V and an X (in the manner shown in Figure 4). The energy of the second configuration per unit length of the original PGB is $2(\frac{1}{\cos(\frac{\pi}{4}+\frac{\varphi}{2})}) \cdot \sin^3(\frac{\pi}{4}-\frac{\varphi}{2})$ (two new PGBs, each of length $\frac{1}{\cos\frac{\varphi}{4}+\frac{\varphi}{2}}$) or $1-\sin\varphi$. The contribution from the circular contours around the convex disclination is much smaller. Therefore, the VX pair configuration is preferred for $\varphi > \varphi_C \simeq 43^\circ$. This instability and VX pair creation marks a distinct departure from the analogy with elastic surfaces. There $\Theta = h$, the height of the sheet above a given level, is single valued. Moreover, an elastic surface which is bent along a rooftop requires finite energy. On the other hand, a set of parallel rolls at the preferred wavelength requires no energy just because the phase contours are labelled -4π, -2π, 0, -2π, -4π rather than -4π, -2π, 0, 2π, 4π.

(9) We stress the point: the creation of VX pairs results from a phase transition/instability which occurs when two patches with different orientations (made possible by the rotational symmetry) meet at too sharp an angle. Note that even saddle point singularities, the merging of two concave disclinations, for which the PGBs are at angles of 45° with respect to the roll wavevectors, are unstable. Far from equilibrium, saddles will disintegrate into two concave disclinations (see Figure 12 in [14]).

(10) As R approaches zero, the pattern onset value, at a certain $R_0(\varepsilon)$, which depends on ε, the amplitude becomes an active rather than a passive (slaved) order parameter. It combines with the phase to give a complex order parameter and consequently, disclinations, which have double valued $\vec{k}$ values, disappear. The reason is that the complex order parameter $A_1 \exp i\theta$

and its gradient determines $\nabla\theta$ uniquely. Experiments indeed show that they do.

(11) Exact multivalued solutions of the stationary hyperbolic equation $\nabla \cdot \vec{k}B(k) = 0$ have been found using a hodograph transformation [14,15]. When regularized using (5), they give the V (concave) and X (convex) disclinations shown in Figures 2 and 3. The concave disclinations have three PGBs and their energy scales with their size L. The convex disclinations require much less energy, proportional in fact to $\ln L$, where L is their size.

(12) It is a useful exercise to consider the multivalued solutions of $\nabla \cdot \vec{k}B(k) = 0$ when we set $B(k) = 1$. In this case, the constraint that $k = 1$ almost everywhere is lost but the topological structure of the point defects remains the same. Let $\nabla\Theta = \vec{k} = (f, g) = (k\cos\varphi, k\sin\varphi)$ and write $\zeta = \mathrm{re}^{i\alpha} = X + iY$ and $\Theta = \mathrm{Im}\,\frac{2}{3}\zeta^{3/2} = r^{3/2}\sin\frac{3\alpha}{2}$. A little analysis shows $f - ig = r^{1/2}\exp(i\frac{\alpha}{2}) = ke^{-i\varphi}$. Thus $\varphi = -\frac{\alpha}{2}$. As α travels around the defect at $\zeta = 0$, φ twists by $-\pi$. This is the Laplace concave disclination. The Laplace convex disclination is found by setting $\Theta = \mathrm{Im}\ 2\zeta^{1/2}$. The Laplace equation disclinations arise in the theory of quadratic differentials.

(13) Examples of concave and convex disclinations can be seen on fingertips where they are referred to as triradii and loops, respectively.

Nothing in the theory to date precludes $\vec{k}$ being three or higher dimensional. In the section which follows, we examine the possible natures of defects of a string nature in higher dimensions.

3. V and X string defects in three and higher dimensions

One can construct [21] three-dimensional point defect analogues of concave disclinations with a tetrahedral skeleton replacing the two-dimensional triangular one. Here we focus on a different set of objects we call loop disclinations by attaching backbones to the two-dimensional cross sections seen in Figures 2 and 3. Whereas in two dimensions we had exact solutions of the regularized stationary phase diffusion equation

$$\nabla \cdot \vec{k}B(k) + \varepsilon^2\nabla^4\Theta = 0 \tag{12}$$

to describe disclinations and their composites, here we will use its Laplacian analogue described in point 12 of Section 2. But the main ideas should be apparent from a geometrical viewpoint. For the V or concave disclination string, it is clear that a loop which twists by multiples of $\frac{2\pi}{3}$ over the length ℓ of the backbone can be identified with the original cross section. There are two types. In the first we demand a periodicity of the phase $\Theta(X, Y, Z)$ over the period ℓ in which case the labelling of contours is preserved. Consider Figure 2. In the sectors $0 < \alpha < \frac{2\pi}{3}$, $\frac{4\pi}{3} < \alpha < 2\pi$, $\frac{8\pi}{3} < \alpha < \frac{10\pi}{3}$, the phase contours are labelled 0, 2π, 4π so that the arrow on the 'wavevector' $\nabla\Theta = (f, g, h)$ points away from the rays $\alpha = 0, \frac{4\pi}{3}, \frac{8\pi}{3}$. In the complementary sectors $\frac{2\pi}{3} < \alpha < \frac{4\pi}{3}, 2\pi < \alpha < \frac{8\pi}{3}$ and $\frac{10\pi}{3} < \alpha < 4\pi$, they are labelled 0, -2π, -4π. Periodicity of Θ in $(0, \ell)$ requires twists in the triad (f, g, h) of $\frac{4\pi}{3}$. The corresponding loop index is $\frac{2}{3}$, or $-\frac{2}{3}$ if the twist direction is reversed. Such objects we will call pattern up quarks. On the other hand, if we allow solutions Θ which are

antiperiodic, the corresponding index will be $\pm\frac{1}{3}$. We call this a pattern down quark. Similarly, pattern leptons can be constructed by twisting the loop backbone of the X or convex disclination, shown in Figure 3, by $\pm\ 2\pi$. Their index is then ± 1.

It is useful to write down the Laplace equation analogues. For small r, for which we replace the three halves Bessel function $I_{3/2}$ by its small argument limit, a solution Θ, periodic in Z, the backbone coordinate, can be written

$$\Theta = \frac{2}{3} K r^{3/2} \sin\left(\frac{3\alpha}{2} - \frac{n\pi Z}{\ell}\right) \tag{13}$$

where K is a dimensional constant. The wavevector triad f, g, h can be easily calculated to be

$$f - ig = K r^{1/2} \exp i\left(\frac{\alpha}{2} - \frac{n\pi Z}{\ell} - \frac{\pi}{2}\right), \tag{14}$$

$$h = -\frac{2\pi n}{3\ell} K r^{1/2} \sin\left(\frac{3\alpha}{2} - \frac{n\pi Z}{\ell}\right). \tag{15}$$

The choice $n = 2$ (or any even integer) corresponds to a choice of Θ periodic over $0 \le Z \le \ell$; for the choice $n = 1$, Θ is antiperiodic. Writing $f - ig = \sqrt{f^2 + g^2}\exp(-i\varphi)$ gives us

$$\varphi = -\frac{\alpha}{2} + \frac{n\pi Z}{\ell} + \frac{\pi}{2}. \tag{16}$$

Along the contour $Z = \text{constant}$, $0 \le \alpha \le 2\pi$, the twist or change in φ is $-\pi$. Along the contour

$$\alpha = \alpha_0 + \frac{2\pi}{3} t, \quad Z = \frac{\ell}{n} t, \quad r = r_0(\alpha_0), \quad 0 \le t \le n, \tag{17}$$

with constant phase $\Theta = \frac{2}{3} K r_0^{3/2} \sin 3\frac{\alpha_0}{2}$ and constant $h, \varphi = -\frac{\alpha_0}{2} + \frac{\pi}{2} + \frac{2\pi t}{3}$. Its change $[\varphi]$ over $0 \le t \le n$ is equal to $\frac{2\pi n}{3}$. For the choice of periodic Θ over $0 \le Z \le \ell$, n is even with lowest choice $n = 2$. The corresponding index $\frac{1}{2\pi}[\varphi] = \frac{2}{3}$ is the pattern up quark. The anti up quark corresponds to taking $\Theta = \frac{2}{3} K r^{3/2} \sin(\frac{3\alpha}{2} + \frac{n\pi Z}{\ell})$ and following the triad (f, g, h) on the contour $\alpha = \alpha_0 - \frac{2\pi t}{3}, Z = \frac{\ell}{n} t, n = 2$. The choice of Θ antiperiodic over $o \le Z \le \ell$ leads to a lowest choice of $n = 1$ or $n = -1$ and twists of $\pm\ 2\pi/3$, corresponding to indices $\frac{1}{2\pi}[\varphi]$ of the pattern anti down and down quarks. For pattern leptons, we choose $\Theta = 2K r^{1/2} \sin(\frac{\alpha}{2} - \frac{n\pi Z}{\ell})$ for which $f - ig = \sqrt{f^2 + g^2}\exp(-i\varphi) = K r^{1/2} \exp i(-\frac{\alpha}{2} - \frac{n\pi Z}{\ell} - \frac{\pi}{2})$, $h = \frac{2nK\pi r^{1/2}}{\ell} \sin(\frac{\alpha}{2} + \frac{n\pi Z}{\ell})$. The angle φ is $\frac{\alpha}{2} + \frac{n\pi Z}{\ell} + \frac{\pi}{2}$. On the circuit, $Z = \text{constant}$, $0 \le \alpha \le 2\pi$ we obtain the twist π and index $\frac{1}{2}$. On the circuit $\alpha = \alpha_0 - 2\pi t$, $Z = \frac{\ell}{n} t$, $0 \le t \le n$ and $\Theta = 2K r_0^{1/2} \sin(\frac{\alpha_0}{z}) = \text{constant}$, the change $[\varphi]$ in φ is $-2\pi n$. The choice of Θ to be antiperiodic over $0 \le Z \le \ell$ leads to the indices ∓ 1.

The astute reader may, with good cause, dismiss these constructions as purely formal as we have given no information as to how the large distance structures of these objects can meet, merge and meld with the rest of the pattern. In fact, one may very well require more dimensions to embed them into a self-consistent mosaic. Some of these dimensions may be infinite as with their two-dimensional cross sections.

Others, for example the backbone direction may be intrinsically finite. If infinite, we have to give meaning to the choice of ℓ, the backbone length as measured in units of the preferred wavelength.

If one manages to get the topologies of such objects correct, the next task is to ask about their interaction energies and whether they might give rise to familiar force laws. The energies of the pattern quarks increase linearly with their cross sectional diameters L and backbone lengths ℓ. The energies of the pattern leptons increase logarithmically with their cross sectional diameters and linearly with backbone length. The interaction energy would be defined as the difference between their total energies and the sum of their individual energies. While we have not yet managed to calculate any of the interaction energies or their dependencies on the distance r between any such two objects and their 'spin' and 'charge' invariants, we note that there will be a finite interaction energy between V and X loops even if both are untwisted along the backbone direction. So the forces will involve more than their 'charges.'

One might also surmise as to what possible length scales the underlying preferred pattern wavelength might correspond. To this end, we might note that if the angle of merging of the two patterns is just supercritical (see remark 8, Section 2), the singular centres (backbones) of the resulting V and X string are very close, of the order of a pattern wavelength, (see, e.g. the length of the nipples in Figure 7 of [22]). The forces of the 'charged' (i.e. twisted) objects and the 'uncharged' (i.e. untwisted) objects would be comparable. Would the pattern wavelength be the pattern analogue of the Planck length or a quantization of space or space-time? One can also imagine how to make pattern hydrogen atoms. In [22], we show how VX pairs occur in two-dimensional patterns in a large ellipse with boundary conditions chosen to ensure that the local pattern wavevector is parallel to the normal of the elliptical boundary. This corresponds in convection patterns to heating the boundary of a shallow elliptical cylinder. If instead of an elliptical boundary, we were to create a three-dimensional pattern in an ellipsoid with its two largest semi-major axes equal, then their VX nipples would correspond to 'uncharged' neighbouring VX strings.

But such musing and flights of imagination are highly speculative and more than likely destined for the dustbins of history. Nevertheless, it is intriguing that, without any insertions of special symmetries such as SU(2) and SU(3), patterns with the simplest of initial symmetries (translation and rotation) manage, when stressed far from equilibrium, to create them all on their own.

Acknowledgements

This work was supported by NSF grant DMS 0906024 in the proposal for which the notion of pattern quarks and leptons was first suggested.

References

[1] D.J. Griffiths, *Introduction to Elementary Particles*, 2nd ed., Wiley, New York, 2008.
[2] Eberhard Bodenschatz. Private communication.
[3] M. Seul, L. Monar, L. O'Gorman, and R. Wolf, *Morphology and local structure in labyrinthine stripe domain phase*, Science 254 (1991), pp. 1557–1696.

[4] L. Kramer and W. Pesch, *Convection instabilities in nematic liquid crystals*, Ann. Rev. Fluid Mech. 27 (1995), pp. 515–541.
[5] U. Tkalec, M. Ravnik, S. Copar, S. Zumer, and I. Musevic, *Reconfigurable knots and links in chiral nematic colloids*, Science 333 (2011), p. 62.
[6] S. Copar and S. Zumer, *Nematic braids: Topological invariants and rewiring of disclinations*, Phys. Rev. Lett. 106 (2011), pp. 177–801.
[7] A.M. Pertsov, R.R. Allev, and V.I. Krinsky, *Three dimensional twisted vortices in an excitable chemical medium*, Lett. Nat. 345 (1990), p. 419.
[8] R.B. Laughlin, *Anomalous quantum Hall Effect: An incompressible quantum fluid with fractionally charged excitations*, Phys. Rev. Lett. 50 (1983), p. 1395.
[9] H.L. Stormer, *Nobel Lecture: The fractional quantum Hall effect*, Rev. Mod. Phys. 71 (1999), p. 875.
[10] M.C. Cross and P.C. Hohenberg, *Pattern formation outside of equilibrium*, Rev. Mod. Phys. 65(3) (1993), pp. 851–112.
[11] M.C. Cross and A.C. Newell, *Convection patterns in large aspect ratio systems*, Physica D 10 (1984), p. 299.
[12] A.C. Newell, T. Passot, and M. Souli, *The phase diffusion and mean drift equations for convection at finite Rayleigh numbers in large containers*, J. Fluid Mech. 220 (1990), pp. 187–252.
[13] P. Manneville and Y. Pomeau, *Stability and fluctuations of a spatially periodic convections flow*, J. Phys. (Paris) Lett. 40 (1979), pp. 609–612.
[14] T. Passot and A.C. Newell, *Towards a universal theory of patterns*, Physica D 74 (1994), pp. 301–352.
[15] N. Ercolani, R. Indik, A.C. Newell, and T. Passot, *The geometry of the phase diffusion equation*, J. Nonlinear Sci 10 (2000), p. 223.
[16] G.B. Whitham, *Linear and Nonlinear Waves*, Wiley & Sons, New York, 1974.
[17] A.C. Newell and J.A. Whitehead, *Finite bandwidth, finite amplitude convection*, J. Fluid Mech. 38 (1969), pp. 279–303.
[18] L.A. Segel, *Distant side-walls cause slow amplitude modulation of cellular convection*, J. Fluid Mech. 38 (1969), pp. 203–224.
[19] M. Ortiz and G. Gioia, *The morphology and folding patterns of buckling driven thin film blister*, J. Mech. Phys. Solids 42 (1994), pp. 531–559.
[20] F. Bethuel, H. Brezis, and F. Hélein, *Ginzburg-Landau Vortices*, Birkhäuser, Boston, 1994.
[21] Newell A. C., T. Passot, C. Bowman, N.M. Ercolani, and R. Indik, *Defects are weak and self-dual solutions of the Cross–Newell phase diffusion equation for natural patterns*, Physica D 97 (1996), pp. 185–205.
[22] N. Ercolani, R. Indik, A.C. Newell, and T. Passot, *Global description of patterns far from onset: A case study*, Physica D 184 (2003), pp. 127–140.